

Investigation of geometric object and indoor mapping capacity of Apple iPhone 12 Pro LiDAR

Mehmet Akif Günen^{*1}, İlker Erkan², Şener Aliyazıcıoğlu², Cavit Kumaş²

¹Gümüşhane University, Department of Geomatics Engineering, Türkiye

²Gümüşhane University, Department of Mining Engineering, Türkiye

Keywords

iPhone 12 Pro
Point Cloud
LiDAR
Mapping

Research Article

DOI: 10.53093/mephoj.1354998

Received:04.09.2023

Revised: 04.10.2023

Accepted:09.10.2023

Published:17.10.2023



Abstract

LiDAR (light detection and ranging) sensors use laser beams to calculate distances in the surroundings. These sensors can be applied to a wide range of tasks, and they are frequently helpful in tasks like building 3D maps, navigating airplanes, robots, conducting mining operations, and automated driving. High-resolution distance measurements are taken by LiDAR sensors, but they also gather environmental data. This information aids in locating, identifying, and quantifying things and their surroundings. The iPhone 12 Pro, which Apple released in 2020, was evaluated for accuracy with various geometric shapes and its capacity to recognize indoor environments. Free of charge 3D Scanner and the Clirio Scan application were employed in this situation. However, it was found that the root mean square error and mean error in indoor mapping were ± 1.41 cm and -0.56 cm in 3D Scanner and ± 3.94 cm and -0.60 cm in the Clirio Scan application, respectively, despite the findings obtained showing low accuracy in scanning small geometric objects due to the scanning difficulty. Clirio does not reject the null hypothesis in the t-test that was conducted. The accuracy of the LiDAR sensor in indoor mapping has been shown to be more promising than that of small items. In order to evaluate the reliability and reusability of the indoor mapping application according to reference measurements, intraclass correlation test was performed and the results were determined to be reliable.

1. Introduction

Terrestrial laser scanning, aerial laser scanning, structured light, structure-from-motion, and multi-view stereo are photogrammetric data acquisition approaches that will help various fields [1-4]. Rapid breakthroughs in image and signal processing techniques, as well as technological microchip advancements, have enabled the production of low-cost and minimum sensors. These methods have advantages and weaknesses, and new generation technologies are expected to make data collecting faster and more flexible. It is also critical to conduct accurate research on newly created technology. Close range remote sensing technologies such as Light Detection and Ranging (LiDAR) are creating greater opportunities than ever for architectural surveying [5], forensic [6], restoration [7], archaeological documentation [8], underground mining operations [9], mining and post mining operations [10-12], game character modeling, analysis and interpretation [13]. LiDAR technology is now widely employed in geomatic applications due to its speed, practicability, and

precision. Data capture for LiDAR typically uses the time-of-flight (ToF) and phase difference methods. This technology, particularly when combined with the Inertial Measurement Units (IMU) system, has cleared the path for its application in a variety of disciplines [14]. This allows for the rapid creation of 3D point clouds and models. Involving a larger number of non-expert users in the process assures that the augmented reality application and documentation process of the created models is widely disseminated throughout the community, highlighting the need of investigating LiDAR/photogrammetric systems. Development of micro-dimensions of sensors and electro-mechanical components lead to support these systems with high computational power. This digital advancement has been aided by different technology advances, resulting in a broader use for the 3D documentation process [14-18].

Although LiDAR technology has long been utilized in terrestrial laser scanning, it is not always practicable to retrieve, preserve, and transport these instruments, and operating them requires expertise. The widespread use of electronics products has reduced the cost to the

* Corresponding Author

(akif@erciyes.edu.tr) ORCID ID 0000-0001-5164-375X
(ilkererkan@gumushane.edu.tr) ORCID ID 0000-0001-7326-6297
(s.aliyazicioglu@gumushane.edu.tr) ORCID ID 0000-0002-5177-8221
(ckumas@gumushane.edu.tr) ORCID ID 0000-0002-4221-3034

Cite this article

Günen, M. A., Erkan, İ., Aliyazıcıoğlu, Ş., & Kumaş, C. (2023). Investigation of geometric object and indoor mapping capacity of Apple iPhone 12 Pro LiDAR. Mersin Photogrammetry Journal, 5(2), 82-89

consumer overall and increased the speed of portable devices like smartphones and tablets, leading to continued advancements in computing power, overall performance, advancements in computer vision algorithms, and general data processing optimizations. In order for the end customer to be able to reverse engineer the product design, the manufacturer competes by delivering high quality products customized to meet their needs. The infrared and RGB sensor of the RGB-D sensors, for instance, are used in a variety of applications, including indoor mapping, 3D mapping and localization, path planning, body tracking, health applications, and Human Pose, despite the fact that they were originally introduced to improve player performance and the sense of realism [1, 19, 20]. The path for the digitization of actual items has been prepared thanks to the LiDAR and TrueDepth technologies integrated into Apple's new devices released in 2020. Being less dependent on the energy source (like heavy batteries) and easily handling related to LiDAR, it is apparent that these devices will be mentioned more for scientific purposes in the upcoming years. Although Apple's LiDAR was mainly created for augmented reality applications, it is important to look into its use in other reverse engineering applications. Using the ToF concept, Apple's LiDAR sensor produces a modulated light signal and detects the time difference with the returning wave, in other word the amount of time it takes for the signal to return in order to measure an object [21-23].

This study was conducted to determine the potential use of LiDAR in the iPhone 12 Pro series as a 3D scanner. The scanning ability of small geometric objects as well as the possibilities for indoor scanning were examined in this context. The measured distances from point clouds obtained with "3D Scanner App" and "Clirio Scan" applications on the Apple Store were compared to the actual value obtained in this scope, and the utility of the LiDAR sensor in geomatic applications was explored using reliability tests.

2. Material and Method

Two different applications from Apple Store were used to obtain point clouds of small items with distinct geometric properties and indoor point clouds encompassing bigger regions with a LiDAR sensor. The actual measurements of the targeted objects were measured five times with a steel tape measure and averaged. Figure 1 presents the sensors of the iPhone 12 Pro used in the fulfillment of this study. The general specifications of the iPhone 12 Pro are as follows: Wide camera: 12 MP, f/1.6, 26 mm, telephoto camera :12 MP, f/2.0, 52 mm and ultrawide camera:12 MP, f/2.4, 13 mm, 120° [24]. It is stated that its ToF LiDAR scans a maximum range of 5 m. Although the main purpose of iPhone LiDAR is to develop digital photo capture, especially in low light focusing, most of software (i.e., Polycam, Heges, EveryPoint, RTAB-MAP, Scaniverse, Clirio Scan, 3D Scanner App, and Pix4DCatch) produces textured 3D scans with the help of Apple ARKit [25]. In addition, since the TrueDepth sensor of iPhone 12 Pro (Figure 1) detects in the infrared region, which located on the front of the phone, it generates data in dark environments, but it is

not the subject of this study. Because of their quick guided acquisition, simple user interface, and reasonably short processing periods that allowed results, the 3D Scanner App and Clirio Scan applications were selected for this study. Although the software works with GPS/GNSS incorporated in outdoor field work, it is turned off in inside work since GPS impacts the accuracy of the data collected. Small item photogrammetric digitization presents a significant challenge in general. Therefore, sphere and cylinder-shaped geometric objects were scanned. Interior mapping of the Gümüşhane University Engineering Faculty (Gümüşhane, Türkiye) corridor was made after examining Apple's new LiDAR, in order to evaluate the system's effectiveness in a bigger region.



Figure 1. Sensors of iPhone 12 Pro.

First, point clouds were produced by scanning the spherical and cylindrical objects shown in Figure 2-3. The spherical object is a desk-mounted educational model of the world globe. The cylindrical item is a laboratory-scale steel grinding tube (Ball Mill Chamber/Grinding Chamber) used in mining engineering laboratory tests. The outside of a model of the world globe was used for spherical shapes, while the interior of the grinding tube (Ball Mill Chamber/Grinding Chamber) was used for cylindrical shapes. The dimensions of the objects are specified at Table 1. When the figures are examined, it is seen that the applications capture different number of point data even though data is taken from different tracking array at the same time. After the point cloud is produced, its transformations to the mesh model are provided. Then, the data was filtered using Taubin's algorithm [26]. The Taubin filter was used because it is a successful method that provides a type of low-pass and high-pass filtering on 3D point clouds or surfaces. By performing the filtering process, noise removal is ensured from the data, so that the inappropriate fit of the models to be fitted to small objects and the measurement process from noisy points in the interior are prevented. The model parameters obtained by fitting the best model to the geometric features were compared with their actual measurements. For indoor mapping, real measurements of 20 different objects were taken from the created point cloud. Matlab 2021a software was used for model fit to geometric shapes, MeshLab for point cloud filtering and measurements of object edges and SPSS 18 software for statistical research. All applications are using MSI delta 15 laptop with AMD Ryzen 9 9500 HX processor, RX6700 graphics card and 32 GB RAM.

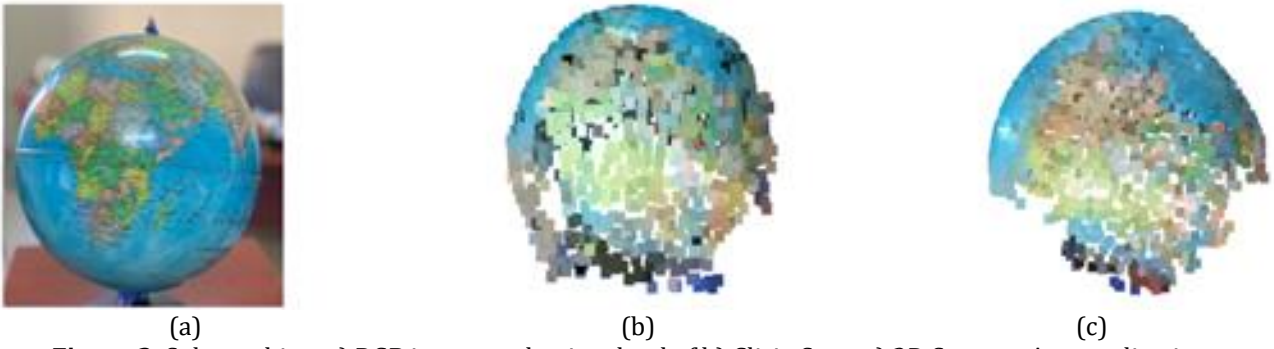


Figure 2. Sphere object a) RGB image, and point cloud of b) Clirio Scan, c) 3D Scanner App applications.

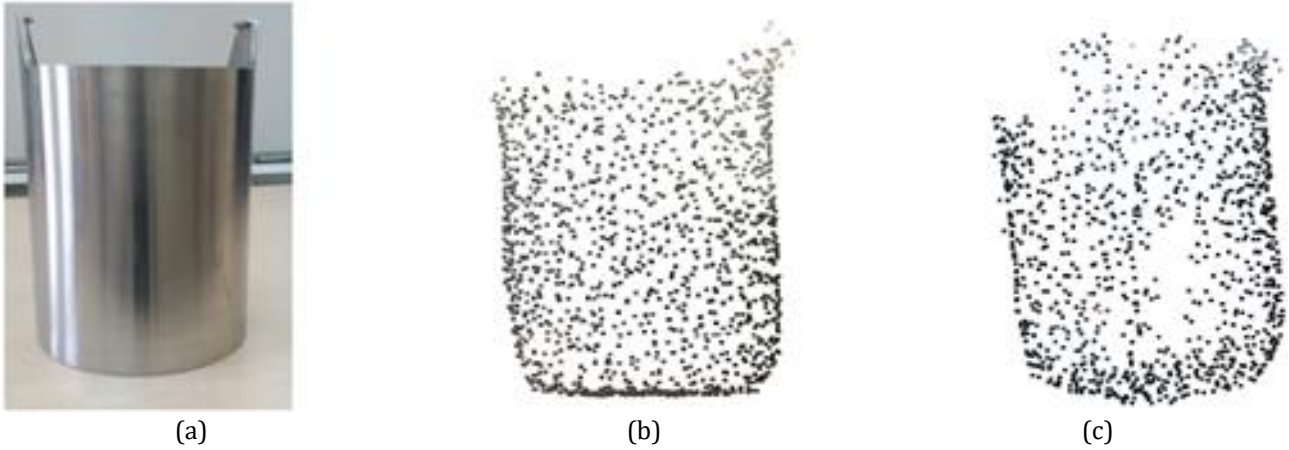


Figure 3. Cylinder object a) RGB image, and point cloud of b) Clirio Scan, c) 3D Scanner application.

3. Results and Discussion

In the application, firstly, objects with spherical and cylindrical shapes were scanned using Clirio Scan and 3D Scanner App applications. Examining the objects presented in point clouds [Figure 2](#) and [Figure 3](#), it is seen that the objects scanned with Clirio Scan have a higher number of points but contain more noise. The best fit model results fitted to the obtained point clouds are presented in [Table 1](#) and their visual representations from different perspectives are presented in [Figures 4-5](#).

The actual area of the modeled cylinder is 2,401.31 cm² and its volume is 1,810.12 cm³. The area calculated with Clirio Scan is 2,416.25 cm² and the volume is 1,838.4 cm³, and the area calculated with the 3D Scanner is

2,382.56 cm² and the volume is 1,843.79 cm³. From this, it can be deduced that both Clirio Scan and 3D Scanner App detects the area with a difference of under 1% while Clirio Scan gives the nearest. When it comes to the volume of the cylinder the difference is increased and both applications detect the volume of the cylinder with a difference of between 1.5-1.9% while Clirio Scan is still gives the nearest.

The actual volume of the modeled sphere is 13,884.22 cm³ and its surface area is 2,793.61 cm². The volume calculated with Clirio Scan is 10,374.85 cm³ surface area is 2,300.41 cm², the volume calculated with 3D Scanner App is 11,273.79 cm³ surface area is 2,431.44 cm². It can be seen once more that the point cloud created by the 3D Scanner App provides values that are closer.

Table 1. Best fit model and actual measurement results.

Application Name	Model	
	Cylinder Actual Height: 29.7 cm Actual Radius: 9.7 cm	Sphere Actual Radius:14.91
Clirio Scan	Height: 30.51 cm Radius: 9.59 cm	Radius:13.53
3D Scanner App	Height:31.69 cm Radius:9.26 cm	Radius:13.91

The procedure of indoor mapping was carried out after the identification of small geometric objects. [Figure 6](#) shows the locations of the assets measured in the scanned corridor, and [Table 2](#) lists the numerical results of the associated measurements. Measurements were taken in this context for the nameplate, the corridor

width, the corridor length, the column length, the poster length, and different tables.

[Figure 7](#) shows the information on the differences between the lengths estimated with MeshLab software over the point clouds created by the applications and the steel tape measure accepted as the actual value. Since the

scanning is happening quickly, it can be claimed that the greatest size disparities between the two applications typically occur in the direction of camera movement.

Because moving quickly can lead to the data being misalignment.

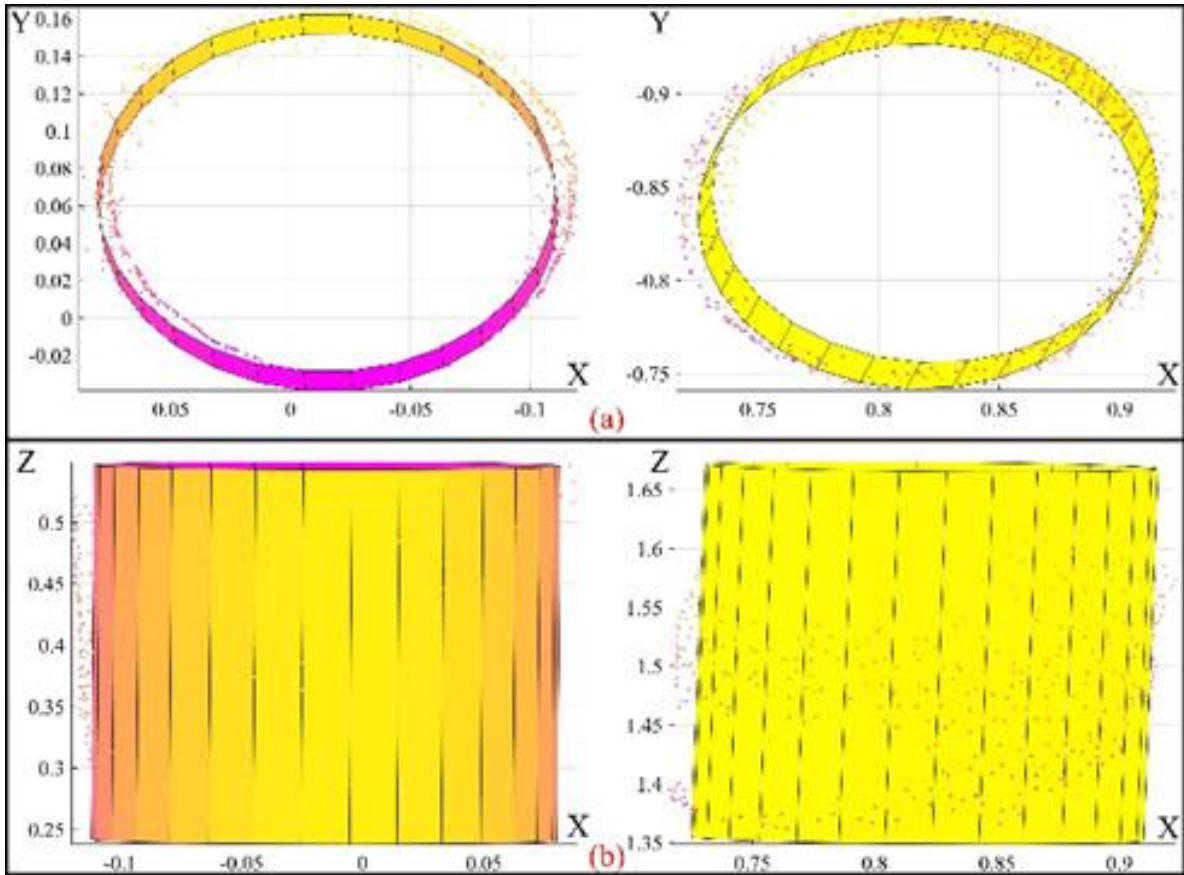


Figure 4. Cylinder fitted to a) 3d Scanner App data b) Clirio Scan data from different viewpoints.

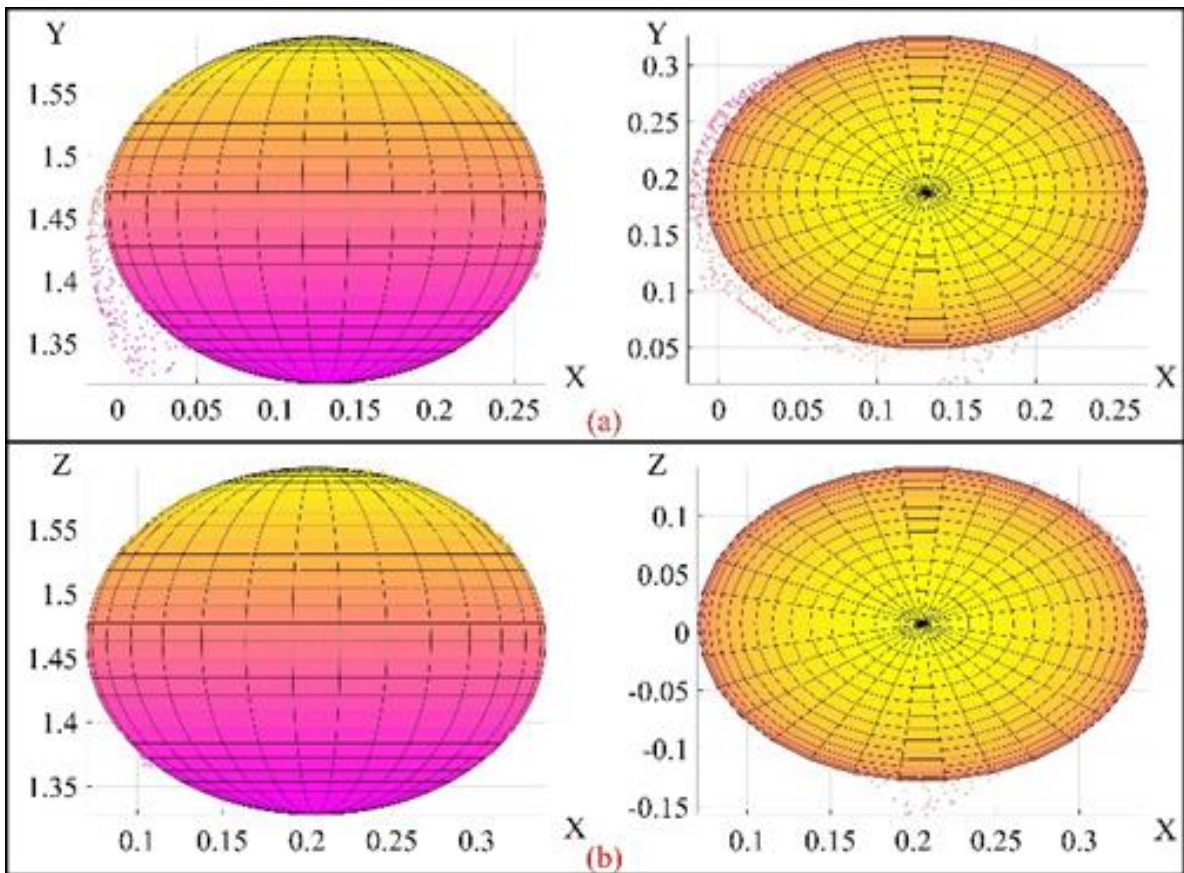


Figure 5. Sphere fitted to a) 3D Scanner App data b) Clirio Scan data from different viewpoints.

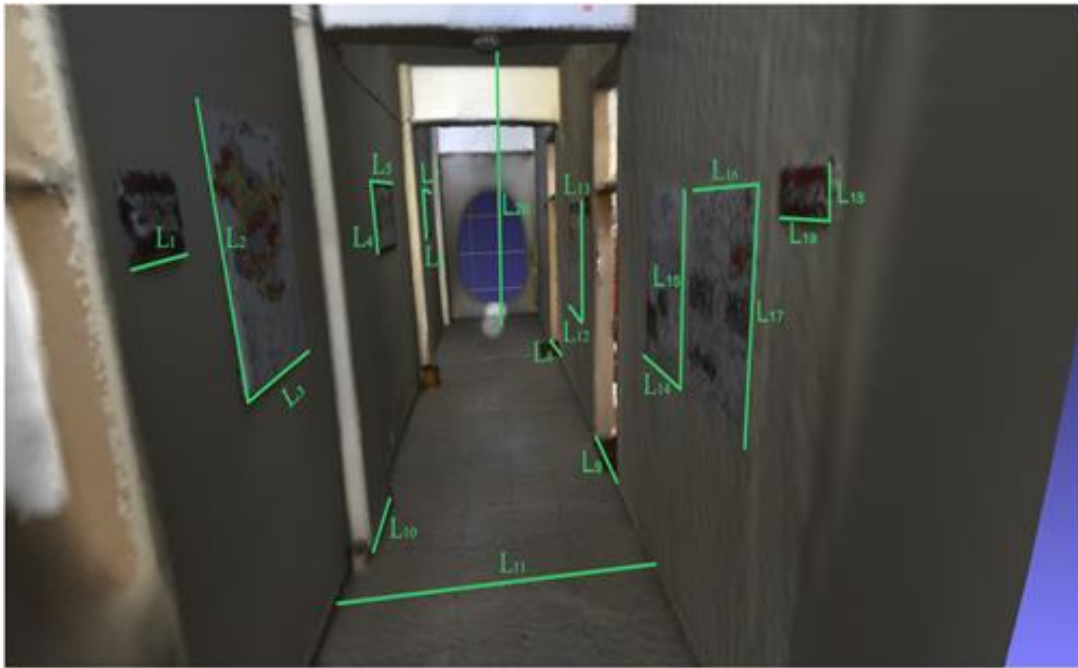


Figure 6. Display of the measured objects on the mesh model.

Table 2. Actual and application-generated point cloud measurements.

#Lengths	Actual value (cm)	3D Scanner value (cm)	Clirio Scan value (cm)
L1	25.3	25.43	25.67
L2	95.4	97.21	93.62
L3	66.0	66.02	66.78
L4	52.5	52.35	52.89
L5	92.5	93.89	95.38
L6	62.4	61.01	62.65
L7	84.3	84.59	85.47
L8	80.6	81.56	77.85
L9	80.7	81.05	82.60
L10	56.3	59.82	59.66
L11	217.5	217.86	217.76
L12	91.0	90.65	94.79
L13	121.5	122.43	121.10
L14	59.5	60.66	64.65
L15	84.7	86.78	83.31
L16	59.5	60.38	59.30
L17	84.7	85.17	83.28
L18	12.0	12.24	12.74
L19	25.3	24.59	24.40
L20	330.02	329.31	329.73

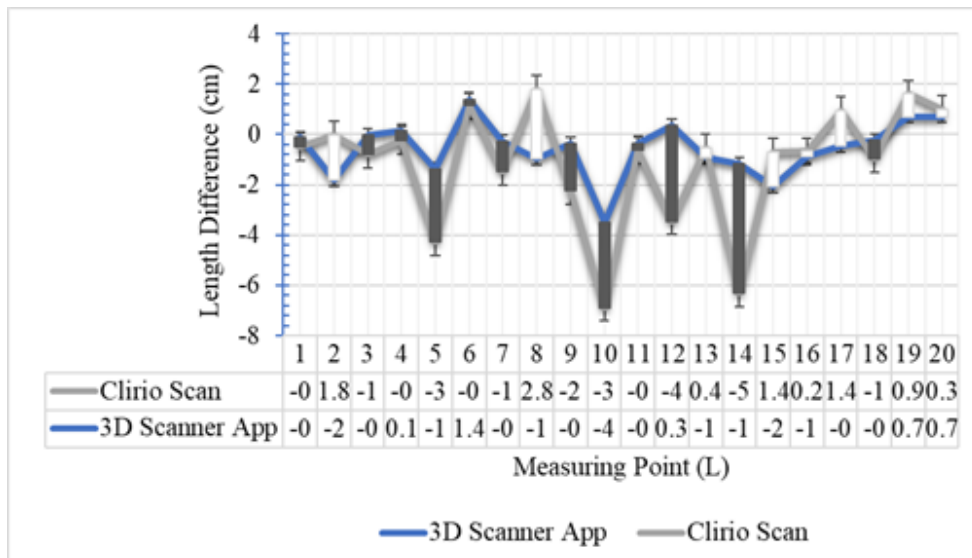


Figure 7. Differences in length between estimated and actual values.

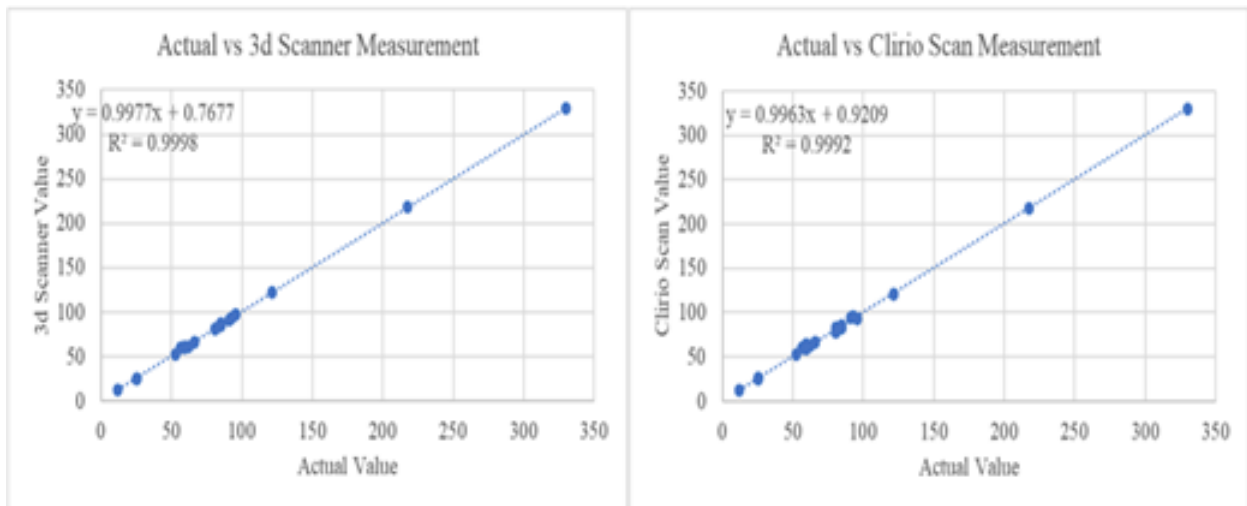


Figure 8. Linear trend model of actual measurements vs 3D Scanner App, and actual measurements vs Clirio Scan application.

When the information is examined, it is seen that the biggest difference occurs in the L_{14} length in the point cloud produced by the Clirio Scan software, with 5.15 cm, and the lowest difference occurs in the L_1 length by the 3D Scanner App application. Linear trend model of actual measurements vs Clirio Scan and actual measurements vs 3D Scanner App application values are given in Figure 8.

In statistical analysis processes, regression analysis is one of the most popular techniques. There are multiple dependent variables that have an impact on the dependent variable. The established model's performance was assessed using the R^2 . The lower the total square of the residuals, in R^2 , which measures the regression's goodness of fit, the better the fit. R^2 is always between 0 and 1, and the closer it is to 1 in general, the more variability the model can explain. The data obtained from the relevant applications are related to the actual values since the R^2 value obtained from the applications in the performed study is greater than 99%.

To determine the data's statistical significance for indoor mapping, the paired sample t-test was used. The pairwise difference between actual data and software-generated data vectors is compared to test the null hypothesis that it has a mean of zero. The null hypothesis is not rejected by the data from Clirio Scan ($p=0.198$), but it is by the results from the 3D Scanner App ($p=0.034$). Small values of p raise questions about the reliability of the null hypothesis since they increase the probability of observing a test statistic. Apple only describes the 5 m range of the LiDAR sensor used in its products; no other feature descriptions are provided. This restricts the application's use to regions larger than 5 m² and to big areas. Application has a limitation because of this. Though it has a restricted capacity, the program strives to provide the best performance it can and gets better with each passing day. It receives upgrades almost weekly. The major issue with the software is misalignment because it doesn't provide accurate trajectory tracking and doesn't react quickly. A different

issue from these is the development of data gaps as a result of starting and continuing from various starting locations. It takes knowledge to collect data because of this. Although these black box applications provide filtered data while exporting the data, the noise levels of the data obtained by using the Taubin's filter are further lowered to fit the most suitable geometric models and make the length measurement more precise.

The intraclass correlation coefficient (widely used for reliability index), which has a value between 0 and 1, is a descriptive statistic that can be employed when quantitative measurements are taken on units grouped in groups. It expresses correlations inside a data class rather than correlations between two independent data classes.

4. Conclusion

The accuracy of the Apple iPhone 12 Pro's LiDAR scanner was investigated in this study. Real measurements were compared with scans of various geometric shapes and interior mapping. The scanning of small geometric objects is fairly challenging, but the results are very encouraging as a result of the findings. Especially on cylinder shaped model Clirio Scan gives the closest values while 3D Scanner App is a little less accurate. The values detected for spherical model showed that the 3D Scanner App detected the model relatively accurate. Since the detected values for both applications are in range of 13-25% difference 3D Scanner App detected the sphere more accurate than Clirio Scan. In terms of indoor mapping, it is highly effective. The sensor's limited capacity to scan over a short distance, however, is a significant drawback. The accuracy of the point cloud the software produces is crucial, according to the statistical tests done. It can be said that 3D Scanner App application produces better results than Clirio Scan. In future studies, accuracy analysis will be carried out by including different software and working on larger areas.

Author contributions

Mehmet Akif Günen: Writing, Investigation, Implementation, **İlker Erkan:** Conceptualization, Validation, Writing, **Şener Aliyazıcıoğlu:** Reviewing, Ideating, Writing, **Cavit Kumaş** Ideating, Language checking, Editing the manuscript

Conflicts of interest

The authors declare no conflicts of interest.

References

- Günen, M. A., & Beşdok, E. (2021). Comparison of point cloud filtering methods with data acquired by photogrammetric method and RGB-D sensors. *International Journal of Engineering and Geosciences*, 6(3), 125-135. <https://doi.org/10.26833/ijeg.731129>
- Guo, B., Zhang, Y., Gao, J., Li, C., & Hu, Y. (2022, September). SGLBP: Subgraph-based local binary patterns for feature extraction on point clouds. *Computer Graphics Forum*, 41(6), 51-66. <https://doi.org/10.1111/cgf.14500>
- Seyfeli, S., & OK, A. (2022). Classification of mobile laser scanning data with geometric features and cylindrical neighborhood. *Baltic Journal of Modern Computing*, 10(2), 209-223. <https://doi.org/10.22364/bjmc.2022.10.2.08>
- Silva, M. F., Green, A., Morales, J., Meyerhofer, P., Yang, Y., Figueiredo, E., ... & Mascareñas, D. (2022). 3D structural vibration identification from dynamic point clouds. *Mechanical Systems and Signal Processing*, 166, 108352. <https://doi.org/10.1016/j.ymssp.2021.108352>
- Nex, F., & Rinaudo, F. (2009). New integration approach of photogrammetric and LIDAR techniques for architectural surveys. *The International Archives of the Photogrammetry, Remote Sensing and Spatial Information Sciences*, 38(3), 12-17
- Bahirat, K., & Prabhakaran, B. (2017). A study on lidar data forensics. *IEEE International Conference on Multimedia and Expo (ICME)*, 679-684. <https://doi.org/10.1109/ICME.2017.8019395>
- Almeida, D. R. A. D., Stark, S. C., Chazdon, R., Nelson, B. W., César, R. G., Meli, P., ... & Brancalion, P. H. S. (2019). The effectiveness of lidar remote sensing for monitoring forest cover attributes and landscape restoration. *Forest Ecology and Management*, 438, 34-43. <https://doi.org/10.1016/j.foreco.2019.02.002>
- Lozić, E., & Štular, B. (2021). Documentation of archaeology-specific workflow for airborne LiDAR data processing. *Geosciences*, 11(1), 26. <https://doi.org/10.3390/geosciences11010026>
- Leottau, D. L., Vallejos, P., & del Solar, J. R. (2018). LIDAR-based displacement estimation in mining applications. *6th International Congress on Automation in Mining*. 1-9
- Froese, C. R., & Mei, S. (2008). Mapping and monitoring coal mine subsidence using LiDAR and InSAR. *GeoEdmonton*, 8, 1127-1133.
- Kekeç, B., Bilim, N., Karakaya, E., & Ghiloufi, D. (2021). Applications of terrestrial laser scanning (TLS) in mining: A review. *Türkiye Lidar Dergisi*, 3(1), 31-38. <https://doi.org/10.51946/melid.927270>
- Murray, X., Apan, A., Deo, R., & Maraseni, T. (2022). Rapid assessment of mine rehabilitation areas with airborne LiDAR and deep learning: bauxite strip mining in Queensland, Australia. *Geocarto International*, 37(26), 11223-11252. <https://doi.org/10.1080/10106049.2022.2048902>
- Günen, M. A., Çoruh, L., & Beşdok, E. (2017). Oyun dünyasında model ve doku üretiminde fotogrametri kullanımı. *Geomatik*, 2(2), 86-93. <https://doi.org/10.29128/geomatik.318319>
- Horand, R., Hansard, M., Evangelidis, G., & Ménier, C. (2016). An overview of depth cameras and range scanners based on time-of-flight technologies. *Machine vision and applications*, 27(7), 1005-1020. <https://doi.org/10.1007/s00138-016-0784-4>
- Zhang, P., He, H., Wang, Y., Liu, Y., Lin, H., Guo, L., & Yang, W. (2022). 3D urban buildings extraction based on airborne lidar and photogrammetric point cloud fusion according to U-Net deep learning model segmentation. *IEEE Access*, 10, 20889-20897. <https://doi.org/10.1109/ACCESS.2022.3152744>
- Zeybek, M., & Ediz, D. (2022). Detection of road distress with mobile phone LiDAR sensors. *Advanced Lidar*, 2(2), 48-53.
- Karkinli, A. E. (2023). Detection of object boundary from point cloud by using multi-population based differential evolution algorithm. *Neural Computing and Applications*, 35(7), 5193-5206. <https://doi.org/10.1007/s00521-022-07969-w>
- Aliyazıcıoğlu, Ş., Öztürk, K. F., & Günen, M. A. (2023). Analysis of Gümüşhane-Trabzon highway slope static and dynamic behavior using point cloud data. *Advanced Lidar*, 3(1), 70-75.
- Günen, M. A., Kesikoğlu, A., Karkinli, A. E., & Beşdok, E. (2017). RGB-D sensörler ile iç mekan haritalaması. *International Artificial Intelligence and Data Processing Symposium (IDAP)*, 1-6. <https://doi.org/10.1109/IDAP.2017.8090220>
- Kadkhodamohammadi, A., Gangi, A., de Mathelin, M., & Padoy, N. (2017). A multi-view RGB-D approach for human pose estimation in operating rooms. *IEEE winter conference on applications of computer vision (WACV)*, 363-372. <https://doi.org/10.1109/WACV.2017.47>
- Vogt, M., Rips, A., & Emmelmann, C. (2021). Comparison of iPad Pro®'s LiDAR and TrueDepth capabilities with an industrial 3D scanning solution. *Technologies*, 9(2), 25. <https://doi.org/10.3390/technologies9020025>
- Teppati Losè, L., Spreafico, A., Chiabrando, F., & Giulio Tonolo, F. (2022). Apple LiDAR Sensor for 3D Surveying: Tests and Results in the Cultural Heritage Domain. *Remote Sensing*, 14(17), 4157. <https://doi.org/10.3390/rs14174157>
- Kuçak, R. A., Erol, S., & Alkan, R. M. (2023). iPad Pro LiDAR sensörünün profesyonel bir yersel lazer tarayıcı ile karşılaştırmalı performans analizi. *Geomatik*, 8(1), 35-41.

<https://doi.org/10.29128/geomatik.1105048>
24. https://support.apple.com/kb/SP831?locale=en_US
25. <https://developer.apple.com/augmented-reality/arkit/>

26. Taubin, G. (1995). A signal processing approach to fair surface design. in Proceedings of the 22nd annual conference on Computer graphics and interactive techniques. 351-358



© Author(s) 2023. This work is distributed under <https://creativecommons.org/licenses/by-sa/4.0/>